Traction control of a Formula Student prototype

André Filipe Alves Grancho Barroso
andre.g.barroso@tecnico.ulisboa.pt

Instituto Superior Técnico, Universidade de Lisboa, Lisboa, Portugal

September 2021

Abstract

Controlling tire slip is crucial for race cars performance, such as Formula Student prototypes. The high power-to-weight ratio, longitudinal and lateral accelerations, coupled with relatively short wheelbase and track width, results in significant dynamic mass transfers. A traction control system must handle nonlinearities and be robust to parametric changes or uncertainties to improve dynamic vehicle behaviour. To fulfil these requirements, a cascade control architecture based on proportional control and tire dynamics is proposed, being able to simultaneously fulfil longitudinal (accelerating and decelerating) and lateral (turning) dynamics requirements. A feedback component is employed to track the longitudinal speed and fulfil tire and electric motor constraints, while a feedforward term is used to track the yaw rate and achieve torque vectoring in turns. Both components improve the vehicle ability to accelerate, decelerate and turn, mitigating the natural tendency to break traction in vertically unloaded tires due to mass transfers. A power distribution module corrects the individual torque commands to enforce electrical power limits in acceleration and deceleration. A heuristic method is suggested to tune the traction control parameters. The sensitivity of the resulting traction controllers is studied for varying traction conditions and vehicle parameters, assessing the proposed solution's robustness. Finally, the traction controllers are validated on generic race tracks, with a higher degree of complexity from the benchmarks used for tuning.

Keywords: Formula Student Driverless, traction control, vehicle dynamics, cascade control

1. Introduction

1.1. Motivation

Traction control systems (TCS) regulate the wheel rotations of ground vehicles, avoiding extreme situations, such as wheel lock an wheel spin. Wheel lock occurs frequently during hard braking manoeuvres, if the applied braking force exceeds a critical value, stopping the wheel and causing tire skid. Conversely, wheel spin can occur at any point when there is excess driving power or poor traction conditions. Both extreme cases must be avoided since they may create unstable driving situations and decrease the effective driving/braking forces, thus resulting in vehicle performance degradation or even loss of control.

FST Lisboa is a team of students from Instituto Superior Técnico, who are passionate about motorsports and engineering. The team was created in 2001 and initially designed race cars with internal combustion engines (ICEV). A shift was made to prototypes with electric powertrains (EV) in 2011, when the team introduced the first electric racing prototype made in Portugal. 2021 was the first year when two prototypes were simultaneously developed: a driverless (DV) and a person-driven one. The future prototype, for the 2022 season, will be a hybrid race car in the sense of having person-driven and driverless configurations that can be mounted according to the type of dynamic event the team wishes to participate in. To extract more dynamic performance from the future hybrid vehicle, this work proposes an approach for traction control that can be applied to both vehicle configurations. In the scope of this thesis, the driverless category is considered in greater detail, since it possesses a higher degree of complexity and richness in terms of vehicle control than the person-driven one.

1.2. Traction control systems

A racing driver, or a computer emulating the driver, is able to produce two major sorts of inputs to drive a car: accelerator/brake pedal input and steering wheel input. Following this logic, a TCS encompasses two categories: longitudinal and lateral control. The longitudinal controller monitors tire adhesion to prevent wheel lock and spin, while the lateral one deals with vehicle behaviour in turns, also referred to as the yaw motion [10]. To implement traction control, one is typically interested in regulating tire slip, defined by the slip ratio κ. Even though there are several definitions for the slip ratio [14], which will be formally defined in section

2.1.2, it can be generally thought of as the relative linear speed between the tires and vehicle centre of gravity (CG). If the former is higher, the vehicle should be accelerating, otherwise deceleration occurs. Tire and vehicle dynamics are nonlinear and have time-varying parameters, reasons why TC algorithms must be robust with respect to nonlinearities and parametric uncertainties [1] [19].

TCS are implemented differently according to the types of powertrain. For vehicles with internal combustion powertrains, TC can be achieved by engine control (air and fuel flow regulation, spark-timing shift), brake control (independent brake actuation) or torque transfer (a fraction of the available torque can be transferred to a wheel with better traction via differentials or clutches) [10]. Vehicles with electric powertrains, especially those with independent motors, present a good opportunity for the application of more sophisticated TC algorithms. Comparing with ICEV, EV have a much faster and precise torque response (in the region of hundredths of seconds [10]), the torque is easily measured knowing the motor current, and the possibility of having independent in-wheel motors enables decoupled wheel torque control [9] [7] [11]. For the EV case, since electric machines can also work as generators, acceleration and deceleration can both be performed without an additional braking system, implying that TC can be realised using only software [10], with the added benefit of battery recharge while braking. In both ICEV and EV, traction control also aims to improve energetic efficiency by limiting wheel slip [1] [20].

Several approaches have been considered to implement TC, the most obvious one being the attempt to realise optimal slip ratio controls according to a tire model such as the Magic Formula [16], however this strategy is not sufficiently sensitive to changing tire-road conditions and results in poor control performance [1]. Commercial TCS are typically designed for the worst-case scenarios that the vehicle might encounter - such as icy road conditions with old tires - which generally results in a suboptimal solution [1] [11] [20], certainly not suitable for a racing application. An approach that incorporates robustness to nonlinearities and parameter variability in its formulation is sliding-mode control, in which the control action may change structure under varying operating conditions, being robust to parameter variations and bounded disturbances [19] [18]. Another approach for TC is an online estimation of the maximum transmissible torque, as demonstrated in [20] and [12]. According to [5], the presence of nonlinearities, parameter variations and state constraints discourages the use of optimal control strategies. The employment of neuro-fuzzy control schemes is also a possibility, as shown in [18], where the unknown nonlinear slip dynamics are approximated by a neural network, robust to modelling inaccuracies; and in [11], where a fuzzy-logic controller is able to compensate for the complex nonlinear tire-road behaviour and adapt to varying road surfaces.

TCS for Formula Student prototypes are not implemented as in most commercially available vehicles, since the typical single-wheel/independent modelling does not accurately capture the coupling and interaction between wheels, due to the high accelerations and mass transfers that the Formula Student vehicles experience [4]. Regarding the advancements proposed by former members of FST Lisboa, several vehicle control strategies were explored in the last decade. Lateral control strategies for FSD were studied in [3], which consisted in a decoupled approach between lateral and longitudinal dynamics that did not consider tire slip for the latter. An ABS for a Formula Student prototype used a cascade control architecture with a proportional-integrative-derivative-fuzzy controller for slip ratio on the outer loop and a brake pressure proportional-derivative controller for the inner loop [6]. From a data-driven perspective, a dynamic vehicle model generated using data from physical vehicle testing with a neural network was used as the prediction model for a nonlinear model predictive controller [8]. A torque vectoring control scheme proposed for a rear-wheel driven (RWD) prototype emulates a mechanical differential to improve handling, using optimal control strategies for yaw rate and lateral velocity tracking [2]. Other Formula Student teams have proposed a linear-quadratic-regulator-integrative approach to regulate traction of a 4WD vehicle [4] and a method to control a RWD prototype that includes both open and closed-loop components to control the relative slip between front and rear wheels [13].

This thesis aims to implement a traction control scheme for an electric Formula Student prototype where longitudinal and lateral dynamics are coupled, aiming to improve vehicle performance in the dynamic events of the Formula Student competitions.

1.3. Objectives

The traction control system, also termed a low-level controller, will work downstream from a high-level controller (if the vehicle is in driverless mode) or a driver (if the vehicle is piloted), which effectively navigate the vehicle on the race track. The low-level controller must regulate the actuation effort in order to ensure vehicle stability and avoid wheel lock and spin. To design and implement the traction control system, the following logic steps and intermediate objectives are defined:

- Research about traction control strategies and understand the mechanisms that govern tire-road interaction;
- Implement a realistic vehicle model that simulates the behaviour of a Formula Student vehicle, including a sufficiently complex tire model, that adequately captures the nonlinear tire behaviour;
- Design traction controllers based on simplified vehicle models and test their validity against the realistic vehicle model;
- Develop a control architecture capable of influencing both longitudinal and lateral vehicle dynamics, while fulfilling tire and powertrain constraints;
- Tune the proposed traction controllers for simple driving benchmarks using a heuristic method;
- Validate the resulting solution for two generic Formula Student Driverless race tracks.

2. Vehicle modelling

Since the controller design, tuning and validation processes are made resorting to simulation, it is important to develop models that emulate the vehicle behaviour. In this section, two vehicle models are detailed, the first of which has a high degree of complexity, being used for simulation, and the second is a simplified single-track model used for control design and preliminary validation of the control architecture.

2.1. Realistic vehicle model

The vehicle model used for simulation has six degrees of freedom (DOF), modelling the vehicle as a rigid body with a simplified vertical suspension system for each wheel. The car is four-wheel-driven (4WD) by independent electric motors and front-wheel steered. Figure 1 shows a schematic of the resulting vehicle model, including the location and orientation of the reference frames, suspension systems and inputs (in green).

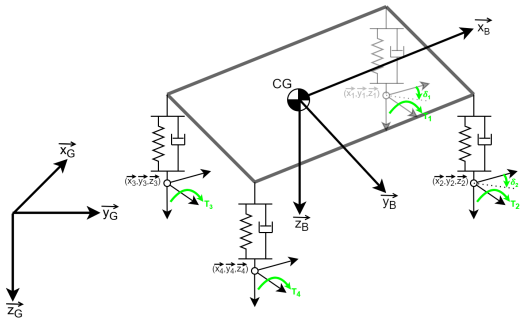

Figure 1: Schematic of the realistic vehicle model.

The vehicle model is formulated in a state-space representation [15], expressed by:

$$\dot{x}(t) = f(x(t), u(t)); \tag{1}$$

$$y(t) = h(x(t), u(t)); \tag{2}$$

in which x is the state vector, u the input vector and y the output vector, as defined in equations (3)-(5). The system output vector y includes both the state vector x and some additional outputs related to the employed tire model that are useful in simulation. The nonlinear vector functions f and h describe the system state and output, respectively.

$$x(t) = (V\ \Omega\ P_G\ \Phi\ \omega)^T; \tag{3}$$

$$u(t) = (T\ \delta)^T; \tag{4}$$

$$y(t) = (V\ \Omega\ P_G\ \Phi\ \omega\ \Delta\ \kappa\ \alpha\ F_x\ F_y\ F_z\ M_z\ T_z)^T. \tag{5}$$

Regarding the input vector u, it combines the four wheel torques (T) and the steering wheel angle (δ). The output vector y encompasses: linear CG velocity (V); angular CG velocity (Ω); CG position (P_G); Euler angles (Φ); wheel angular speeds (ω); suspension systems deformation (Δ); tire slip ratios (κ); tire slip angles (α); longitudinal (F_x), lateral (F_y) and vertical (F_z) tire forces; self-aligning tire moments (M_z) and vehicle yawing torque (T_z).

2.1.1 Dynamics equations

The dynamics equations can be derived according to the Newton-Euler formulation, applied on the CG translation (6), CG rotation (7) and wheels rotation (8):

$$m\ \dot{\vec{V}}(t) = -m\ (\vec{\omega}(t) \times \vec{V}(t)) + m\ S(t)\ \vec{g} + \sum \vec{F}_{CG}(t); \tag{6}$$

$$J_{CG}\ \dot{\vec{\Omega}}(t) = -(\vec{\Omega}(t) \times J_{CG}\ \vec{\Omega}(t)) + \sum \vec{T}_{CG}(t); \tag{7}$$

$$J_w\ \dot{\omega}(t) = T(t) - F_x(t)\ R + \sum T_w(t). \tag{8}$$

Considering equation (6), m is the vehicle mass, $\vec{g}$ is the gravity vector, S is a rotation matrix, and $\vec{F}_{CG}$ is the vector of resultant forces acting on the CG, which includes tire, dissipation and aerodynamics forces. Both dissipation and aerodynamics forces are proportional to $||\vec{V}||^2$. Regarding equation (7), J_{CG} is the CG inertia tensor and $\vec{T}_{CG}$ is the vector of resultant torques acting on the CG, introducing energy dissipation proportional to $||\vec{\Omega}||^2$. Finally, in equation (8), J_w is the wheel rotational inertia and T_w is the wheel dissipation torque, proportional to $||\omega||^2$.

The planar tire forces and moments generation is detailed in the following section, which is influenced by the vertical force acting on each tire. A simplified suspension model is used in this work, aligned with the rigid-body assumption: each suspension

quarter has an equivalent linear spring-damper system that is directly actuated and normal to the ground plane. For this suspension model, the vertical force is given by

$$F_z(t) = \frac{k}{MR^2}\ \Delta(t) + \frac{c}{MR^2}\ \dot{\Delta}(t); \tag{9}$$

in which k and c are the elastic and damping coefficients of the linear spring-damper systems, respectively. The motion ratio MR is the ratio between wheel displacement and equivalent spring/damper system displacement [6].

2.1.2 Tire modelling

FST Lisboa's tire supplier is Continental AG, who provides the C19 racing tires (Competition Tire 2019), including documentation to simulate tire behaviour. Continental AG makes available the treated data from private testing, using the Magic Formula tire model, a semi-empirical model that calculates steady-state tire loads [17] [16]. The semi-empirical classification is given since the model is based on test data, but is also described by physical properties. To be able to employ the provided tire model and compute the friction loads it produces in the tire/road interface, several concepts must be defined. For a free-rolling wheel, as shown in figure 2, with linear velocity $V_w = (V_x\ V_y\ V_z)^T$ measured at the wheel centre, rotating at angular speed ω_0, the tire effective radius R is given by

$$R = \frac{V_x}{\omega_0}. \tag{10}$$

If a driving torque T is applied, a longitudinal tire slip κ occurs,

$$\kappa(t) = -\frac{V_x(t) - R\ \omega(t)}{V_x(t)}, \tag{11}$$

known as the slip ratio, arising from the deformations of the rubber as it contacts the road. This particular formulation implies that $\kappa \to \infty$ if the wheel is spinning (in a tire burnout, for instance) and $\kappa = -1$ if it is locked (under hard braking). Tire slip can also occur laterally if $V_y \neq 0$ and is defined in terms of the side slip angle α,

$$\alpha(t) = \arctan\left(-\frac{V_y(t)}{V_x(t)}\right). \tag{12}$$

The friction coefficient μ is defined as the ratio between longitudinal/lateral force and vertical load:

$$\mu_x = \frac{F_x}{F_z}; \tag{13}$$

$$\mu_y = \frac{F_y}{F_z}; \tag{14}$$

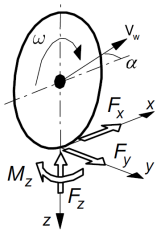

Figure 2: Schematic of a tire and generated forces/moment [16].

and depends on tire-road traction conditions. One can consider, for simplicity,

$$\mu = \mu_x = \mu_y; \tag{15}$$

corresponding to isotropic levels of traction in terms of F_x and F_y.

The tire model provided by Continental AG is valid within the boundaries defined in table 1, which covers a wide range of possible operating conditions.

Table 1: Boundaries of the parameters used in the tire model.

Parameter	Min. value	Max. value
Vertical load (F_z)	230 [N]	1600 [N]
Slip ratio (κ)	−0.25 [-]	0.25 [-]
Slip angle (α)	−0.20 [rad]	0.20 [rad]

Pure longitudinal slip ($\alpha = 0$ [rad]) and pure lateral slip ($\kappa = 0$ [-]) represent the driving scenarios where only one of the slip quantities varies. Having defined the concepts associated with tire mechanics, it is now possible to state the formula that baptises the model. Indeed, for provided values of vertical load F_z and friction coefficient μ, the Magic Formula can be expressed as [16]

$$\begin{aligned} y(x(t)) = D\ \sin(C\ \arctan(B\ x(t) \\ -E(B\ x(t) - \arctan(B\ x(t))))). \end{aligned} \tag{16}$$

The input variable is X, which can be κ or α, and the output variable is Y, which can be F_x, F_y or M_z. To compute F_x, the input variable is κ; to compute F_y and M_z the input variable is α. B, C, D and E are fixed coefficients for provided (F_z, μ) conditions: stiffness factor, shape factor, peak value and curvature factor, respectively.

2.1.3 Powertrain modelling

FST Lisboa employ electric powertrains with in-wheel motors, which may run as four-wheel-driven (4WD) or rear-wheel driven (RWD). For both configurations, the motors are permanent-magnet, synchronous machines (PMSM), characterized in table

2. Each motor is independently controlled in speed-control operating mode, which allows a dynamic limitation of both speed and torque references.

Table 2: Electric motor characterisation from a mechanical standpoint.

Parameter	Symbol	Value, [units]
Nominal speed	N_{nom}	12000 [rpm]
Nominal torque	T_{nom}	10 [N.m]
Nominal power	P_{nom}	12.3 [kW]
Maximum speed	N_{max}	20000 [rpm]
Maximum torque	T_{max}	21 [N.m]
Maximum power	P_{max}	35 [kW]

The electric motors spin at extremely high speeds with relatively low torques, so a gear reduction is necessary. FST Lisboa use a planetary gear train with a fixed gear ratio, $GR = 16.25$ [-], such that the torque at wheel i is given by

$$T_{w_i}(t) = T_{m_i}(t)\ GR. \tag{17}$$

Conversely, the angular speed of wheel i is given by

$$\omega_i(t) = \frac{\omega_{m_i}(t)}{GR}. \tag{18}$$

Since the numerical modelling of the PMSM is outside the scope of this thesis, the torque response dynamics are approximated by a first-order system:

$$G_{PT}(s) = \frac{\eta_{PT}}{t_{PT}s + 1}, \tag{19}$$

where $\eta_{PT} = 0.90$ [-] is the equivalent powertrain efficiency that considers the accumulator, inverters, electrical connections and drivetrain (considered constant); $t_{PT} = 0.02$ [s] is the time constant of the torque dynamics.

2.1.4 Steering modelling

The rotation of a steering wheel or an actuator - in the driverless case - induces a steering angle in the tires. FST Lisboa's vehicles are only front-wheel steered. From a kinematics perspective, if both front tires are steered by the same angular amount, the outer tire would start skidding, since the radius of curvature that each wheel must describe is different. To allow for $\delta_1 \neq \delta_2$ and consequently avoid tire skid, the Ackermann steering geometry may be employed, a principle applicable to low-speed/low curvature curves [14], such as the ones found in typical Formula Student race tracks. The steering of a Formula Student prototype is not direct, which means that the steering wheel has a higher rotation than that of the tires $i = 1, 2$. Formally, $SR > 1$ [-], with the steering ratio being defined as

$$SR = \frac{\delta(t)}{\delta_i(t)}. \tag{20}$$

According to the Ackermann steering geometry, the steering angles δ_1 and δ_2 can be computed as:

$$\delta_1(t) = \arctan\left(\frac{(L_f + L_r)\tan(\delta(t)/SR)}{L_f + L_r - \frac{L_t}{2}\tan(\delta(t)/SR)}\right); \tag{21}$$

$$\delta_2(t) = \arctan\left(\frac{(L_f + L_r)\tan(\delta(t)/SR)}{L_f + L_r + \frac{L_t}{2}\tan(\delta(t)/SR)}\right); \tag{22}$$

in which L_f, L_r and L_t are the distance from the CG to the front axle, from the CG to the rear axle, and the track width, respectively.

Similarly to the powertrain modelling, the steering angle actuation is also modelled as a first-order system as

$$G_{STA}(s) = \frac{1}{SR\ (t_{STA}s + 1)}, \tag{23}$$

where $t_{STA} = 0.1$ [s] is the steering actuation time constant.

2.2. Simplified vehicle model

The vehicle model used for control design is an extension of the dynamic bicycle one. To capture the tire-road interaction, an additional state - tire slip ratio κ - is introduced, analogous to a unicycle model, which is directly influenced by the input motor torque T_m. Additionally, a yawing moment due to torque vectoring T_{TV} is also considered as an input and included in the yaw rate equilibrium equation. The model, summarised in equations (24)-(27) represents a RWD car with longitudinal and lateral tire slip dynamics, front-wheel steering and torque vectoring possibility. The tire forces are computed using a simplified Magic Formula formulation.

$$\begin{aligned}\dot{u}(t) = \frac{1}{m}(&-F_{y_f}(t)\ \sin(\delta_f(t)) + F_{x_r}(t) \\ &-C_t\ u^2(t)) + v(t)\ r(t);\end{aligned} \tag{24}$$

$$\begin{aligned}\dot{\kappa}(t) = \frac{R}{J_w\ u(t)}&\left(-\frac{F_{x_r}(t)}{2}\ R + T_m(t)\ GR\right) \\ &-\frac{\dot{u}(t)}{u(t)}(1 + \kappa(t));\end{aligned} \tag{25}$$

$$\dot{v}(t) = \frac{1}{m}(F_{y_f}(t)\ \cos(\delta_f(t)) + F_{y_r}(t)) - u(t)\ r(t); \tag{26}$$

$$\dot{r}(t) = \frac{1}{I_{zz}}(F_{y_f}(t)\ \cos(\delta_f(t))L_f - F_{y_r}(t)\ L_r + T_{TV}(t)). \tag{27}$$

$$F_{x_r}(t) = \frac{2\ m\ g}{4}\ \sin(1.9\ \arctan(20\ \kappa(t))); \quad (28)$$

$$F_{y_f}(t) = -\frac{2\ m\ g}{4}\ \sin(2.2\ \arctan(10\ \alpha_f(t))); \quad (29)$$

$$F_{y_r}(t) = -\frac{2\ m\ g}{4}\ \sin(2.2\ \arctan(10\ \alpha_r(t))); \quad (30)$$

If the state (1) and output (2) equations are linearised about the operating state, the linearised state-space representation is obtained [15]:

$$\dot{x}(t) = A(t)\ x(t) + B(t)\ u(t); \quad (31)$$

$$y(t) = C(t)\ x(t) + D(t)\ u(t); \quad (32)$$

where A is the state matrix, B the input matrix, C the output matrix and D the direct transmission matrix.

As shown in equations (24)-(27), the model has $x(t) = (u\ \kappa\ v\ r)^T$ as state vector and $u(t) = (T_m\ T_z\ \delta)^T$ as input vector. To define the control strategy, the model was linearised around a trim point which corresponds to expected operating conditions of the vehicle on a regular basis. The corresponding linear, time-invariant state-space representation is:

$$\begin{pmatrix} \dot{u}(t) \\ \dot{\kappa}(t) \\ \dot{v}(t) \\ \dot{r}(t) \end{pmatrix} = \begin{pmatrix} A_{11} & A_{12} & 0 & 0 \\ A_{21} & A_{22} & 0 & 0 \\ 0 & 0 & A_{33} & A_{34} \\ 0 & 0 & A_{43} & A_{44} \end{pmatrix} \begin{pmatrix} u(t) \\ \kappa(t) \\ v(t) \\ r(t) \end{pmatrix} + \begin{pmatrix} 0 & 0 & 0 \\ B_{21} & 0 & 0 \\ 0 & 0 & B_{33} \\ 0 & B_{42} & B_{43} \end{pmatrix} \begin{pmatrix} T_m(t) \\ T_{TV}(t) \\ \delta(t) \end{pmatrix}; \quad (33)$$

The linearisation results show that the vehicle model can be divided into two decoupled subsystems:

- Longitudinal subsystem (analogous to the unicycle model): the motor torque T_m directly influences the wheel slip ratio κ which, in turn, influences the longitudinal speed u - a chained system. The dominant (slower) closed-loop pole is associated to the longitudinal vehicle speed, whereas the one associated to the tire slip ratio is five orders of magnitude faster.
- Lateral subsystem (analogous to a pure lateral model): the steering angle δ directly affects the lateral speed v and yaw rate r, with a smaller contribution from the yawing moment due to torque vectoring T_{TV} for the latter. The eigenvalues of the subsystem's A matrix show the same order of magnitude in terms of closed-loop pole locations. The dominant (slightly slower) pole is associated to the yaw rate dynamics.

Both subsystems are closed-loop stable, as well as the resulting system, since all eigenvalues have negative real components.

3. Traction control of a Formula Student protyptype

3.1. Simplified vehicle model implementation

To develop a traction control architecture that is able to simultaneously influence longitudinal (accelerating and decelerating) and lateral (turning) dynamics, it is useful to analyse the vehicle model derived in the previous section, particularly the consequences of the linearised model:

- The longitudinal and lateral subsystems are decoupled, suggesting the employment of two independent controllers.
- The longitudinal dynamics is chained: the motor torque influences the tire slip ratio, which in turn influences the vehicle longitudinal speed. The slip ratio dynamics is several orders of magnitude faster than that of the longitudinal vehicle speed.
- The lateral vehicle speed and the yaw rate dynamics are coupled, with the latter being slower. The yawing torque due to torque vectoring directly affects the yaw rate dynamics.

These learnings justify the implementation of the longitudinal and lateral controllers for the simplified vehicle model, which can be summarised by the diagram from figure 3.

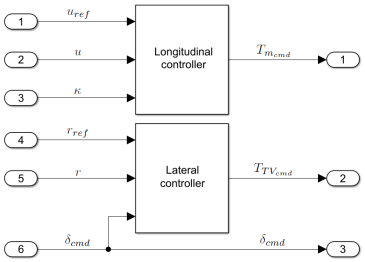

Figure 3: Block diagram of the simplified traction control scheme.

A cascade control architecture for the longitudinal subsystem is suggested, allowing the control of both the slip ratio κ (inner loop) and the longitudinal speed u (outer loop). This structure is appropriate for the longitudinal traction control problem due to the existing coupling of the slip ratio and the longitudinal speed dynamics and since the former is faster - they can be controlled in chain. This architecture also allows the controller to directly saturate the physical quantities that must be limited: the slip ratio κ must be limited due to tire performance constraints (34) and the motor torque command $T_{m_{cmd}}$ is bounded by hardware limits (35):

$$\kappa(t) \in [\kappa_{min}, \kappa_{max}]; \quad (34)$$

$$T_{m_{cmd}}(t) \in [T_{m_{min}}, T_{m_{max}}]. \quad (35)$$

The controllers employed are proportional gains, K_u and K_κ, such that:

$$\kappa_{ref}(t) = K_u(u_{ref}(t) - u(t)); \quad (36)$$

$$T_{m_{cmd}}(t) = K_\kappa(\kappa_{ref}(t) - \kappa(t)). \quad (37)$$

The use of independent wheel-hub motors allows for asymmetric torque distributions. A left/right motor torque asymmetry assists in controlling the slip ratios created in each tire while describing a turn. Additionally, if a left/right torque asymmetry exists, a yawing moment due to torque vectoring $T_{TV_{cmd}}$ will be created, inducing a rotation of the car about the $\vec{z}_B$ axis. In fact, the regulation of the yawing moment is crucial in a typical Formula Student race track with sharp and consecutive turns, in addition to the steering wheel input, allowing the car to rotate on its vertical axis and perform a turn with the highest possible yaw acceleration. Since the yaw rate and lateral vehicle speed are coupled, and given that the regulation of the yawing torque T_z is important, the lateral controller is defined as a yaw rate tracker, creating an additional yawing moment command due to torque vectoring $T_{TV_{cmd}}$, given by

$$T_{TV_{cmd}}(t) = K_r(r_{ref}(t) - r(t)), \quad (38)$$

where K_r is a proportional gain. To observe physical and stability limits, the additional yawing moment is bounded by

$$T_{TV_{cmd}}(t) \in [T_{TV_{min}}, T_{TV_{max}}]. \quad (39)$$

3.2. Realistic vehicle model implementation

The bicycle model with slip dynamics is useful to better understand the requirements and controller architecture. However, being a single-track vehicle model, it is not sensitive to vertical load transfers, which strongly influence the tire deformations - slip ratio and slip angle. Additionally, the RWD simplification with one equivalent motor torque command $T_{m_{cmd}}$ does not physically describe the evolution of T_z - which has contributions from the four existing motors. However, the merits of the proposed control architecture can be extended to the realistic tridimensional vehicle model presented in section 2.1.

Figure 4 shows the proposed full complexity traction controllers, consisting of three modules: longitudinal controller, lateral controller and power distribution. Based on the yaw rate tracking error $e_r = r_{ref} - r$, the lateral controller (figure 6) provides a slip ratio asymmetry κ_{diff} to the longitudinal controller (figure 5), which controls both the individual tire slip ratios κ and the vehicle longitudinal speed u according to the longitudinal speed tracking error $e_u = u_{ref} - u$. After computing the appropriate torque commands for each motor T that simultaneously tracks u_{ref} and r_{ref}, the power distribution module checks whether the commands satisfy the Formula Student regulations and powertrain constraints and appropriately allocates the available electrical power to the four motors, outputting the final commands T_{cmd}, consisting of T_{cmd_1}, T_{cmd_2}, T_{cmd_3} and T_{cmd_4} and δ_{cmd} - which remains unchanged from the input value - that will enter the simulator.

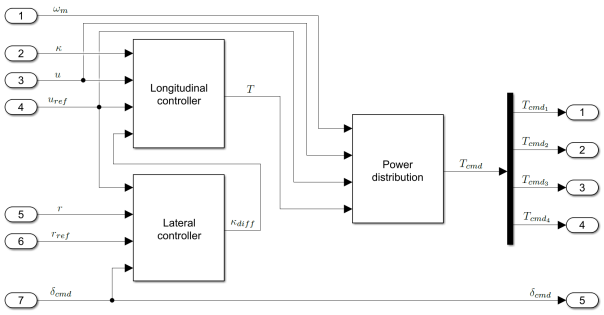

Figure 4: Block diagram of the full complexity traction control scheme.

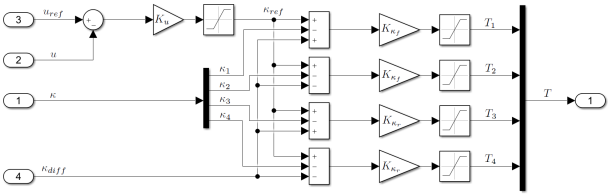

Figure 5: Block diagram of the longitudinal controller.

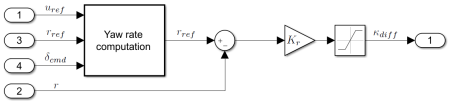

Figure 6: Block diagram of the lateral controller.

4. Controllers tuning and validation

4.1. Formula Student Driverless regulations

There are several dynamic events in a Formula Student competition, with slightly different rules for the person-driven and driverless categories but essentially with common goals. Considering the driverless category regulations, the dynamic events are: Acceleration (seventy five metres straight, followed by a braking zone); Skid Pad (figure-of-eight track, driven at constant speed); Autocross (assesses peak driving performance); Trackdrive (assesses durability and reliability over ten laps of the Autocross track); Efficiency (assesses energy consumption relative to vehicle speed).

To cover a wide range of driving conditions, the traction controllers are assessed in three categories: purely longitudinal, purely lateral and combined. For each category, a performance index J_P is suggested, to evaluate the aspects that are assumed to be more relevant in that category. A heuristic tuning procedure for the traction controllers is suggested in the following sections. Due to the high number of design parameters and the heuristic nature of the procedure, it does not guarantee the determination of an optimal solution, but should steer the trial-and-error process in the correct direction. Further parameter tuning can be performed on-track, starting from the proposed solution this thesis suggests.

4.2. Longitudinal performance

Pure longitudinal performance is heavily influenced by the longitudinal controller and power distribution modules, which have the following design parameters: gains K_u, K_{κ_f} and K_{κ_r}; slip ratio saturations κ_{max} and κ_{min}; motor torque saturations $T_{f_{min}}$, $T_{f_{max}}$, $T_{r_{min}}$ and $T_{r_{max}}$; electrical power limits P_{max} and P_{min}; which correspond to eleven degrees of freedom. To achieve a design parameter combination that improves longitudinal performance, the following steps are followed:

1. Determine the desired range of tire slip by defining κ_{max} (tire slip in acceleration) and κ_{min} (tire slip in deceleration).
2. Determine the desired range of electrical power P_{max} (PMSM in motor mode) and P_{min} (PMSM in generator mode).
3. Tune gains K_u, K_{κ_f} and K_{κ_r} for a scenario in which motor torque saturations do not play an important role, since the power upper and lower bounds of P_{max} and P_{min} are not reached, and traction is the limiting factor for performance. The selected instance is a step in longitudinal speed from 0 to 10 [m/s]. To try to isolate the effects of a cascade architecture, a known and constant slip ratio reference κ_{ref} is considered to determine K_{κ_f} and K_{κ_r}. After defining K_{κ_f} and K_{κ_r}, gain K_u is tuned to achieve the requirements for the outer loop.
4. Tune the motor torque saturations $T_{f_{min}}$, $T_{f_{max}}$, $T_{r_{min}}$ and $T_{r_{max}}$ for a scenario in which motor torque saturations strongly influence performance. The most relevant instance is necessarily the Acceleration event. For the Acceleration event, the longitudinal speed reference u_{ref} is defined as a step with the size of the vehicle's maximum speed, followed by a command to stop after the 75 [m] of the timed run have elapsed. The suggested performance index is simply given by

$$J_P = t_{run} \quad [\text{s}]. \tag{40}$$

5. Assess the proposed solution in terms of robustness to changing or uncertain driving parameters. The considered parameters are:
   - Friction coefficient μ, tested for ± 50 [%] of the design value, with 10 [%] increments;
   - Vehicle mass m, tested for ± 30 [%] of the design value, with 5 [%] increments;
   - Tire radius R, tested for ± 10 [%] of the design value, with 2.5 [%] increments.

4.3. Lateral performance

Pure lateral performance can be assessed in a steady-state cornering manoeuvre such as the Skid Pad event, or as a transient manoeuvre such as a chicane/slalom. To isolate the component of lateral dynamics as much as possible, the tests are performed at constant longitudinal speed u. Tuning the lateral controller is a simpler task than tuning the longitudinal one, since there are fewer parameters: K_r, $\kappa_{diff_{max}}$ and $\kappa_{diff_{min}}$. Due to the coupling between longitudinal and lateral dynamics (a car cannot turn if it is not moving forward), the lateral controller tuning should be performed after the longitudinal controller is set, with a solution that fulfils longitudinal performance requirements. The procedure to tune the lateral controller is the following:

1. Define gain K_u so that the subsequent tests are performed at a prescribed, constant u - even while turning and consequently dissipating energy - and gains K_{κ_f} and K_{κ_r} so that the resulting motor torque reference stays within an admissible range. Determine the appropriate motor torque saturations to investigate lateral dynamics.
2. Determine the desired slip ratio differences $\kappa_{diff_{max}}$ and $\kappa_{diff_{min}}$, which should be equal in absolute value provided there is no preferential turning side.
3. Tune gain K_r based on two representative instances of lateral dynamics: a step input in yaw rate $r_{ref} = 1$ [rad/s] and a chicane - a typical manoeuvre in racing - both performed at constant u.
4. Assess the proposed solution in terms of robustness to changing friction coefficient μ, tested for ± 50 [%] of the design value, with 10 [%] increments.

4.4. Combined performance

Representing a traditional approach to racing, the high-level goal is to minimize the lap time around a generic race track. From a lower-level, traction control perspective, the goal in driving around a generic race track is still to follow the speed references u_{ref} and r_{ref}, while respecting powertrain and tire state constraints. In the Formula Student Driverless competition, the most complex dynamic event is the Trackdrive, for which FST Lisboa provided two race tracks for simulation, the courses from previous competitions held in Germany and Italy. If the design parameters of the traction controllers were well defined by the procedures for longitudinal and lateral performance (independent tuning for both instances), little or no additional tuning effort should be necessary when both instances are combined, in a way, for a generic race track. The suggested procedure to validate the traction controllers on the generic race tracks is the following.

1. Create sets of trajectories that correspond to increasing levels of traction, based on [3]. Three trajectory categories are considered: poor traction (adequate for low μ values), intermediated traction (adequate for intermediate μ values) and excellent traction (adequate for high μ values).
2. Validate the resulting trajectories for varying μ, ± 50 [%] of the design value, with 10 [%] increments.
3. Compute the performance indexes associated to the traction controllers, J_{P_u} and J_{P_r}, defined as

$$J_{P_u} = \text{RMS}(u_{ref} - u); \tag{41}$$

$$J_{P_r} = \text{RMS}(r_{ref} - r); \tag{42}$$

   and t_{lap} [s], the time it takes fo finish the lap. It is expected that t_{lap} is strongly influenced by the trajectory definition and not so much by the performance of the traction controllers.

   The metrics only make physical sense if the vehicle does not drive off-track, keeping within the blue and yellow cones. If the vehicle drives off-track irreversibly, the run is classified as DNF (did not finish), scoring zero points in that particular run.
4. Investigate whether all tire state and powertrain constraints are fulfilled for the entire range of μ.

5. Results and discussion

After performing simulations of an Acceleration event and a chicane (at constant speed) without traction control considerations, one concludes that a Formula Student is not suited to operate close to the tire stability limits without a TCS, particularly for longitudinal motion, due to the high power-to-weight ratio and short dimensions.

Following the procedures summarised in sections 4.2, 4.3 and 4.4, one achieves a robust traction control scheme, capable of adequately following longitudinal speed and yaw rate references while respecting tire state and powertrain constraints, for a wide range of tire-road friction coefficients. In figures 7 and 8 are shown the motor torque commands and effective values and the tire slip ratios for one lap of the Formula Student Germany Trackdrive event.

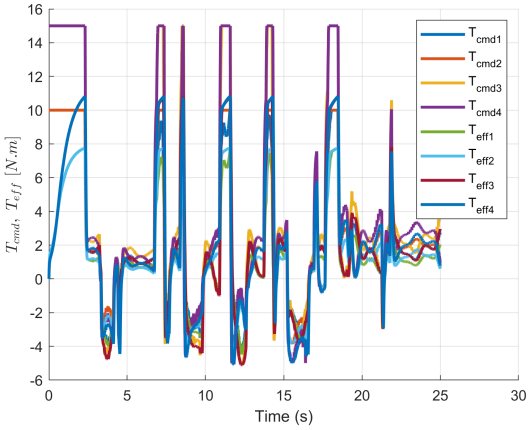

Figure 7: Motor torque commands (T_{cmd}) and effective values (T_{eff}).

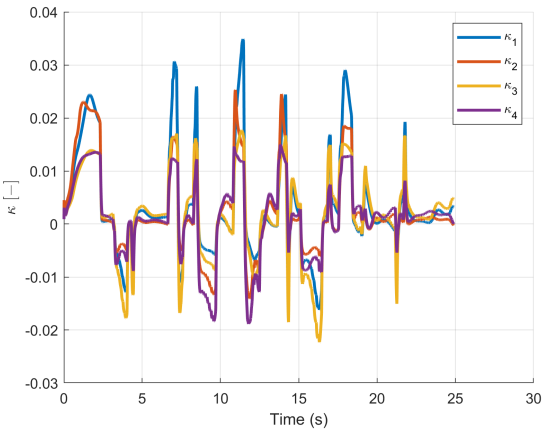

Figure 8: Tire slip ratios (κ).

6. Conclusions

The objetives for this thesis were met, in which a traction control scheme that combines planar dynamics was developed. From the extensive simulation results for varying operating conditions, one concludes that the proposed solution is robust to parametric changes and nonlinearities.

The controller tuning process is made heuristi-

cally, which does not necessarily mean the determination of an optimal solution. The proposed solution may be a starting point to implementing a more generic, optimisation-based, tuning algorithm. Additionally, an accurate modelling of the powertrain electrical components would be beneficial to study its thermal aspects, which limit performance. No sensors are modelled in this work and one assumes all variables of interest are available. In practice, this is not the case, and an estimator should be designed and implemented.

Acknowledgements
The author would like to thank his family, professors Alexandra Moutinho, José Raul Azinheira and Miguel Ayala Botto, as well as Alexandre Athayde and Solange Santos for all the help and encouragement in this work.

References

[1] Fault-tolerant traction control of electric vehicles. *Control Engineering Practice*, 19(2):204–213, 2011.

[2] J. Antunes. Torque vectoring for a formula student prototype. Master's thesis, Instituto Superior Técnico, Universidade de Lisboa, 2017.

[3] A. Athayde. Path following and control for autonomous driving of a formula student car. Master's thesis, Instituto Superior Técnico, Universidade de Lisboa, 2021.

[4] D. Bohl, N. Kariotoglou, A. B. Hempel, P. J. Goulart, and J. Lygeros. Model-based current limiting for traction control of an electric four-wheel drive race car. pages 1981–1986, 2014.

[5] F. Borrelli, A. Bemporad, M. Fodor, and D. Hrovat. An mpc/hybrid system approach to traction control. *IEEE Transactions on Control Systems Technology*, 14(3):541–552, 2006.

[6] J. Ferro. Design and simulation of an abs control scheme for a formula student prototype. Master's thesis, Instituto Superior Técnico, Universidade de Lisboa, 2014.

[7] K. Fujii and H. Fujimoto. Traction control based on slip ratio estimation without detecting vehicle speed for electric vehicle. In *2007 Power Conversion Conference - Nagoya*, pages 688–693, 2007.

[8] H. Furtado. Model predictive control with a neural network model of a formula student prototype. Master's thesis, Instituto Superior Técnico, Universidade de Lisboa, 2020.

[9] T. Furuya, Y. Toyoda, and Y. Hori. Implementation of advanced adhesion control for electric vehicle. In *Proceedings of 4th IEEE International Workshop on Advanced Motion Control - AMC '96 - MIE*, volume 2, pages 430–435 vol.2, 1996.

[10] Y. Hori, Y. Toyoda, and Y. Tsuruoka. Traction control of electric vehicle: basic experimental results using the test ev "uot electric march". *IEEE Transactions on Industry Applications*, 34(5):1131–1138, 1998.

[11] P. Khatun, C. M. Bingham, N. Schofield, and P. H. Mellor. Application of fuzzy control algorithms for electric vehicle antilock braking/traction control systems. *IEEE Transactions on Vehicular Technology*, 52(5):1356–1364, 2003.

[12] S. Ko, J. Ko, S. Lee, J. Cheon, and H. Kim. A study on the road friction coefficient estimation and motor torque control for an in-wheel electric vehicle. *Proceedings of the Institution of Mechanical Engineers, Part D: Journal of Automobile Engineering*, 229(5):611–623, 2015.

[13] J. Loof, I. Besselink, and H. Nijmeijer. Traction control of an electric formula student racing car. In *Proceedings of the FISITA 2014 World Automotive Congress*, 2014.

[14] W. Milliken and D. Milliken. *Race Car Vehicle Dynamics*. SAE International, 1995.

[15] K. Ogata. *Modern Control Engineering*. 2010.

[16] H. Pacejka. *Tire and Vehicle Dynamics*. 2012.

[17] H. B. Pacejka and E. Bakker. The magic formula tyre model. *Vehicle System Dynamics*, 21(sup001):1–18, 1992.

[18] B. Subudhi and S. S. Ge. Sliding-mode-observer-based adaptive slip ratio control for electric and hybrid vehicles. *IEEE Transactions on Intelligent Transportation Systems*, 13(4):1617–1626, 2012.

[19] H. Tan and Y. kwok Chin. Vehicle traction control: Variable-structure control approach. *Journal of Dynamic Systems Measurement and Control-transactions of The Asme*, 113:223–230, 1991.

[20] D. Yin, S. Oh, and Y. Hori. A novel traction control for ev based on maximum transmissible torque estimation. *IEEE Transactions on Industrial Electronics*, 56(6):2086–2094, 2009.